Low temperature failure of bulk nanostructured titanium processed by ECAP

J. Miškuf[1]*, K. Csach[1], A. Juríková[1], V. Ocelík[2], J. Th. M. De Hosson[2], V. Z. Bengus[3], E. D. Tabachnikova[3], A. V. Podolskiy[3], V. V. Stolyarov[4], R. Z. Valiev[5]

[1]*Institute of Experimental Physics, Slovak Academy of Sciences, Watsonova 47, 040 01 Košice, Slovak Republic*
[2]*Department of Applied Physics and Materials Innovation Institute, University of Groningen, Nijenborgh 4, 9747 AG Groningen, The Netherlands*
[3]*B. Verkin Institute for Low-temperature Physics and Engineering UAS, Lenin Avenue 47, 61103 Kharkov, Ukraine*
[4]*A. A. Blagonravov Institute of Mechanical Engineering, RAS, M. Kharitonievsky per. 4, 101 990 Moscow, Russia*
[5]*Institute of Physics of New Materials, Ufa State University, USATU 12, K. Marx Street, 450 000 Ufa, Russia*

Received 19 November 2008, received in revised form 6 February 2009, accepted 3 June 2009

Abstract

Low temperature yield stress and the failure nanostructured titanium of commercial purity produced by severe plastic deformation were analysed. The mechanical properties for specimens with average grain size 15 μm, 0.3 μm and 0.1 μm were studied under uniaxial compression with strain rate $4 \times 10^{-4}\ s^{-1}$ at temperatures 300, 77 and 4.2 K. The failure mechanism was ductile fracture with a preceding formation of an intense shear band. Fractographic analysis revealed "vein" patterns observed at all shear failure surfaces. In a couple of aspects the micromechanism of the shear failure in nanostructured titanium is similar to that in bulk amorphous metallic glasses.

K e y w o r d s: nanostructured titanium, fractography, shear band

1. Introduction

The ductile shear failure under uniaxial tension or compression of some metals consists of the fast sliding of one part of the specimen relative to another (usually along a plane of maximum shear stress) and subsequent ductile rupture [1]. This is caused by the occurrence of a local band of intense adiabatic plastic shear. At present there exist experimental evidences of unstable plastic shear behaviour in nanostructural (NS) titanium [2, 3]. Nanostructured materials comprise of a high density of grains with disordered regions along the grain boundaries, i.e. the system becomes rather disordered. In metallic glasses the presence of the vein pattern morphology at fracture surfaces is caused by meniscus instability, which occurs inside so called liquid-like layer in the vicinity of prefailure catastrophic shear band when the material is locally heated to the quasi-liquid (superplastic) state and it ruptures [4]. The local adiabatic heating to the premelting temperatures in close vicinity of this band is caused by a dissipation of the work produced by the plastic shear. The local heat release is very high due to the near-sound velocity of the shear, the high failure stress and low thermal conductivity of the material [5].

Similar physical conditions exist in the shear band of NS titanium: high failure stresses, nearsonic velocity of plastic shear, and low thermal conductivity of the material. Therefore, the observed "vein" pattern on the shear-failure surfaces of NS titanium can be taken as indirect evidence of high local heating. The discovered "vein" pattern on the failure surfaces of NS titanium possesses some specific features, which are worthy of detailed examination. These are first of all the different quality of "veined" surfaces: they are smooth in some regions (like in metallic glasses) and rough in the others. The present work is focused to the fractographic characterization of failure surfaces of nanostructured titanium at low temperatures, when local heating only occasionally causes microstructural changes.

*Corresponding author: tel.: +421 55 792 2209; fax: +421 55 633 6292; e-mail address: miskuf@saske.sk

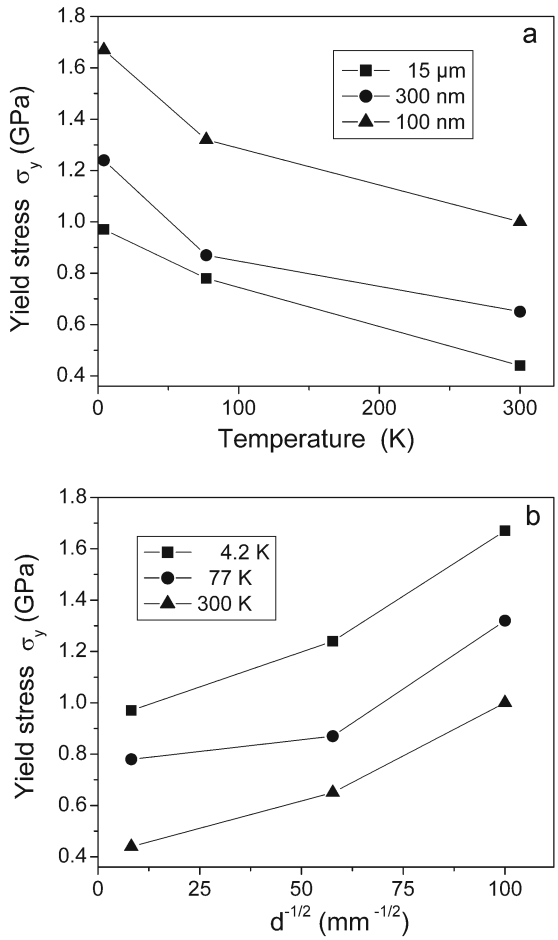

Fig. 1. The yield stress of nanostructured titanium in dependence on the temperature (a) and on the average grain size (b).

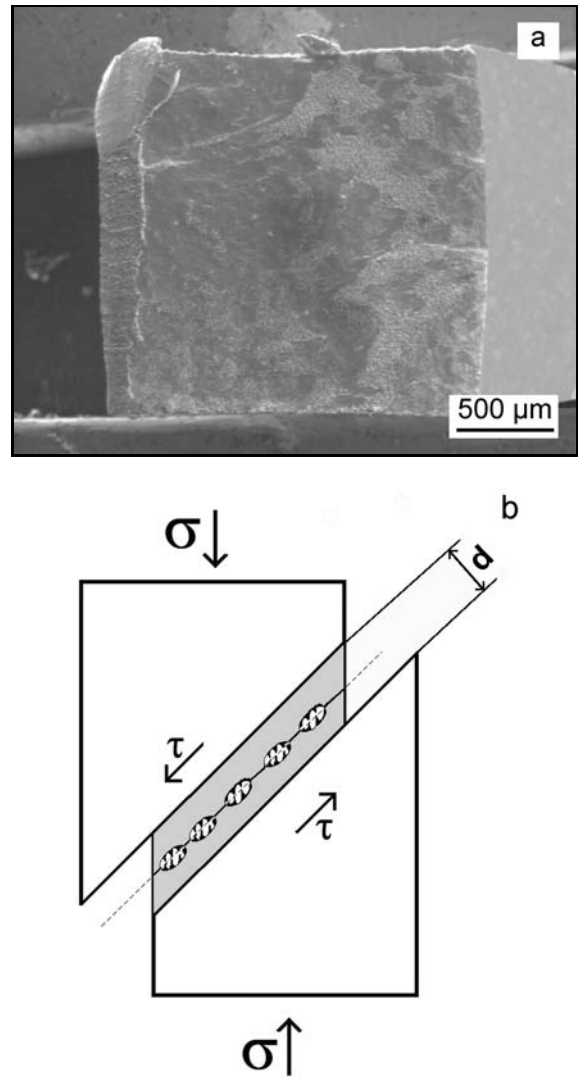

Fig. 2. The top view on fracture surface after the shear failure of nanostructured titanium at 77 K (a) and a scheme of adiabatic shear band formation and its assumed failure (b).

2. Experimental

The investigation was performed on samples cut from 14 × 14 × 160 mm^3 bars of technical-grade VT-1-0 polycrystalline titanium. The deformation and fracture of titanium were studied in three structural states:

– initial state 1 – average grain size $d = 15$ μm, obtained by hot pressing;

– state 2 – average grain size $d = 0.3$ μm, obtained by intense plastic deformation of the initial titanium by means of eight Equal Channel Angular Pressing (ECAP) passes at 450 °C;

– state 3 – average grain size $d = 0.1$ μm, obtained by intense plastic deformation of the initial titanium by eight ECAP passes followed by cold rolling to 75 % deformation, followed by annealing at 300 °C for 1 h.

Mechanical tests were performed on samples characterizing all three material stages under uniaxial compression with constant strain rate of 4×10^{-4} s^{-1} at temperatures of 300 K, 77 K and 4.2 K. The compression axis was parallel to the ECAP axis. Field emission gun scanning electron microscope Philips XL30S operating in secondary electron mode and high-resolution mode as well as confocal optical microscope was used in fractography observations. More details concerning samples preparation and mechanical testing conditions may be found elsewhere [6].

3. Results and discussion

Figure 1 shows the dependence of the yield stress σ_y on the microstructural state and temperature. It is clear from Fig. 1a that the character of the temperature dependence of σ_y remains similar as the grain size varies; the yield stress increases monotonically with decreasing temperature. This dependence shows

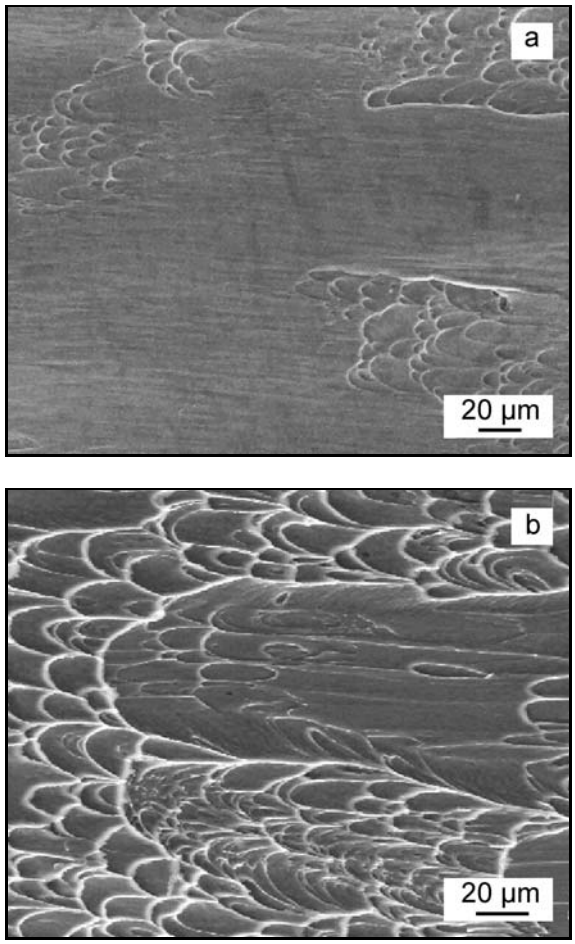

Fig. 3. Alternation of dimpled and smeared regions on the fracture surface of NS titanium failed at 4.2 K (a), dimpled region with elongated different sized dimples (b).

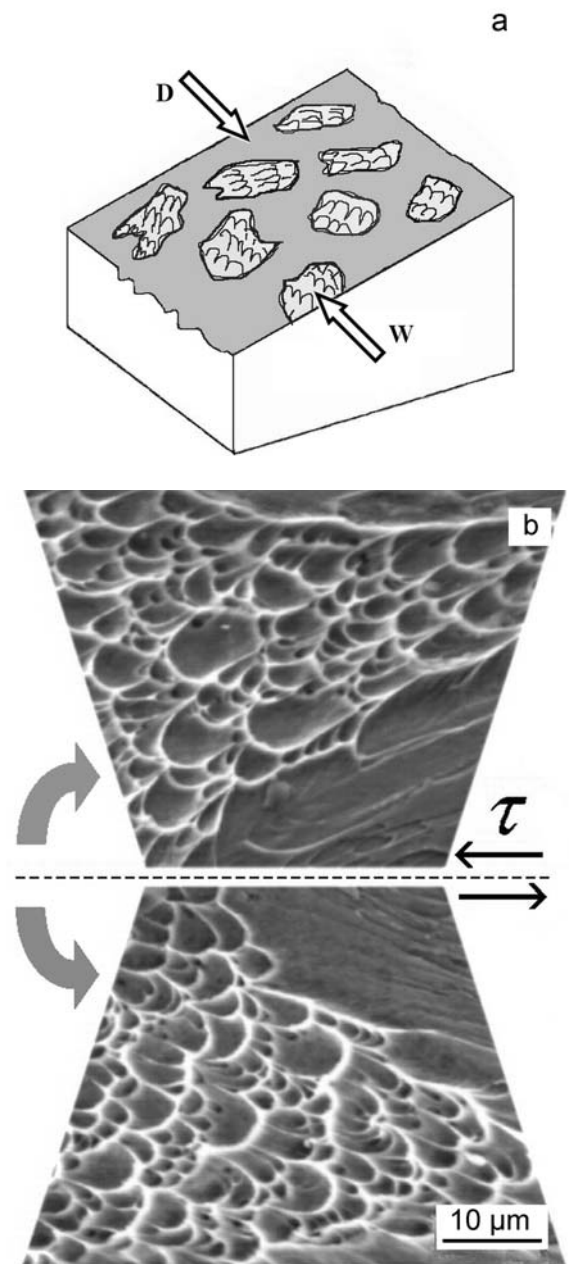

Fig. 4. Scheme of dimpled (W – white) and smeared (D – dark) regions on the fracture surface of NS titanium failed during uniaxial compression (a), dimple morphology on the opposite ductile shear fracture surfaces of NS titanium failed at temperature of 4.2 K (b).

that also in nanostructured titanium the plastic shear events are thermally activated. A similar behaviour is also found in coarse-grained [7] and single crystal titanium [8]. However, hindrance of dislocation sources inside grains in nanocrystalline materials results in preferable nucleation of dislocations at grain boundaries, while the plastic deformation in nanostructured and coarse-grained titanium is mainly realized by intragrain dislocation slip (and twinning at temperatures below 300 K). A tendency to violate well-known Hall-Petch relation for all three temperatures observed may be concluded from Fig. 1b and it indicates the increasing contribution of grain boundary processes to plastic deformation for submicrometer region of grain sizes.

Qualitative fractographic observations have shown only the presence of ductile failure by shear. The ductile failure occurred along a plane of maximum shear stresses. No notable morphology differences between samples failed at different temperatures were observed.

Figure 2 demonstrates macroscopic characteristics of the fracture during uniaxial compression. A macroscopic shear larger than 10 % could be concluded from the presence of its fractographic manifestation on nanostructural sample fractured at 77 K. The fracture surface, along which slipping of one part of a sample relative to another occurred, was oriented at an angle of about 45° to the compression axis as shown in Fig. 2b. The physical conditions for shear band forma-

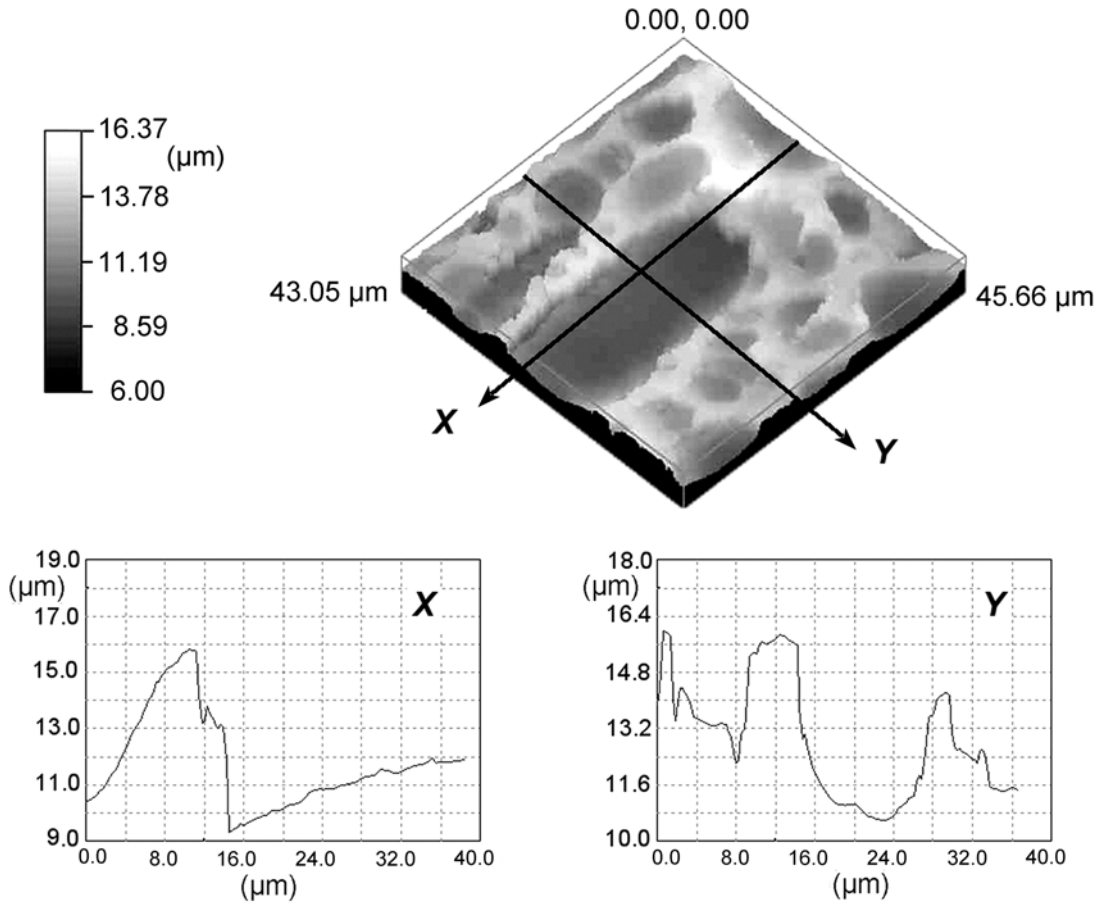

Fig. 5. Confocal microscopy observation of dimples formed on shear failure surface of NS titanium.

tion in nanostructured titanium: the high shear stress, near sound velocity of plastic shear and low thermal diffusivity of the material are similar to the conditions where shear bands are formed in amorphous metallic alloys [5].

The final fracture surface of NS Ti specimens was characterized by (i) the regions of elongated dimples within which no second phase particles were observed, and (ii) the regions with a relatively flat and smeared appearance. These two regions are manifested as white in Fig. 2a, due to the more intense emission of secondary electrons in dimpled areas of fracture surface. Inside the adiabatic shear band area, the shear deformation is so heavy that an identification of microstructural features is not possible. The same is true for nucleation and propagation of cracks.

Figure 3 shows a magnified view on these two areas. Figure 3a shows the fracture surface area where a modulation of dimpled and shear areas occurs. Small ragged areas in the shear direction are visible. Therefore, these regions are believed to be caused by the "gumming" of opposing faces immediately after fracture while the surfaces were still hot due to the high temperature in the shear band region. The closer view to the region of elongated dimples (Fig. 3b) indicates very broad distribution of their size ranging from a micrometer size till tenth of mm. This may be due to the non-uniform distribution of microstructural internal stresses resulting in a scatter of local shear velocities and local heating [6, 9].

Figure 4a shows schematically the alternation of dark (D) and white (W) areas on fracture surfaces of NS titanium samples failed during uniaxial compression. Dimples in each white region are elongated in one direction usually near the direction of macroscopic shear. The SEM images of two opposite fractured surfaces shown in Fig. 4b witness the mirror similarity of dimpled areas and confirm that the final fracture is due to local necking of multiple dimples elongated in the shear direction.

Quantitative analysis of some fractographic features was performed using confocal microscopy. Figure 5 shows a typical result from such observation. The surrounding of 30 μm long and 18 μm wide dimple was observed. 3D fracture surface image and profiles along lines longitudinal (X) and perpendicular (Y) to the macroscopic shear direction are shown in Fig. 5.

The depth of individual dimples is of the order of their lateral dimension (few micrometers) that substantially exceeds the original grain size. It is reason-

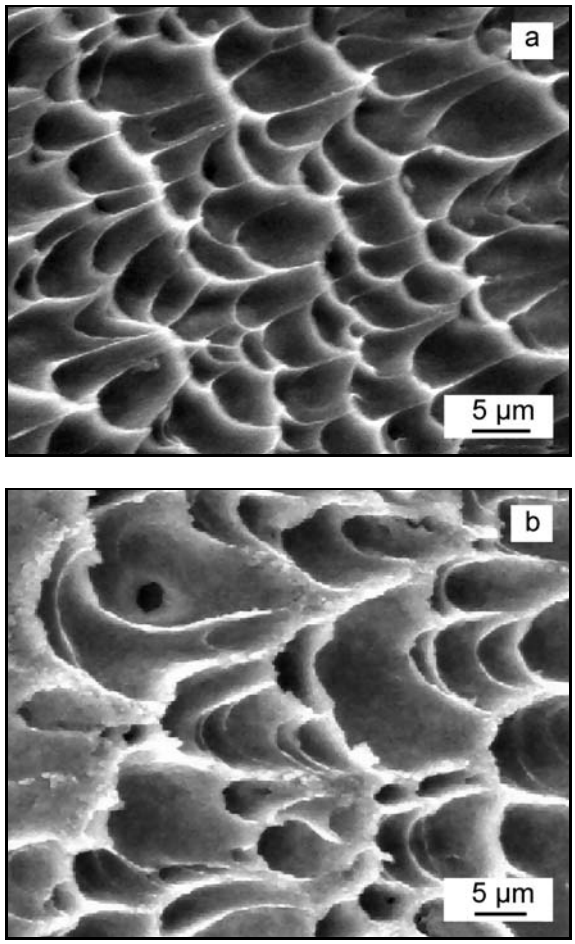

Fig. 6. Morphology of a "vein" pattern on the shear failure surface of NS titanium at 4.2 K: smooth (flat) veins (a) and rough veins (b).

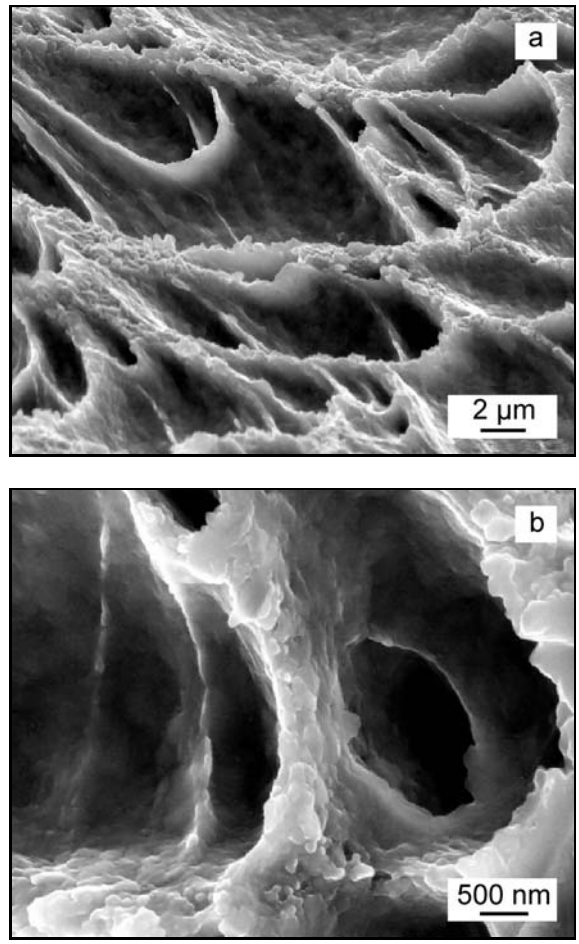

Fig. 7. Mixed (rough and smooth) vein pattern of NS Ti fractured at 77 K (a) and a detail of dimple wall consisting from individual grains or their clusters (b).

able to assume that the value of dimples depth corresponds to the size of the plastic zone d [10], which leads to the conclusion that a collective behaviour of substantial amount of nanostructured grains is involved into shear band formation. Such a collective behaviour has been observed earlier in the Ti6Al4V ELI alloy [11].

As was shown in Fig. 3b one part of the fracture surface of NS titanium is characterized by slightly elongated dimples. It should be noted that we did not observe any inhomogeneities or "secondary particles" that could be qualified as nucleation sites for these dimples. However, Fig. 6 shows two different types of veins around dimples observed at the same fracture surface formed during failure at 4.2 K. In Fig. 6a the smooth veins are shown, similar to these observed at fracture surface of amorphous metallic alloys failed under similar conditions. Even certain indications of local melting are visible on this fracture surface in the form of small globular particles laying on the fracture surface that are considered as an evidence of a melting during last stage of the metallic glass failure [12]. The formation of veins with characteristic rough ridges is shown in Fig. 6b. On the rough veins the "clusters" of small grains are observed. These clusters can be associated with individual original Ti grains or with their aggregates thanks to their corresponding size. In this case the dimples are larger and no evidences of local melting are accompanied.

Figure 7a shows that smooth and rough veins are not always separated to different regions but these two types of veins may coexist in a close neighbourhood. Figure 7b shows a closer view to the rough walls formed around one dimple.

The electron microscopy image of the detail of rough dimple wall made in the high resolution mode has shown that the final width of ragged dimple wall is about 300–400 nm and that the isolated grains as well as grain clusters are visible at "the most latest" fracture surface (Fig. 8). Another interesting feature frequently present on the ragged dimple walls is their perforation before the final failure occurs. This feature

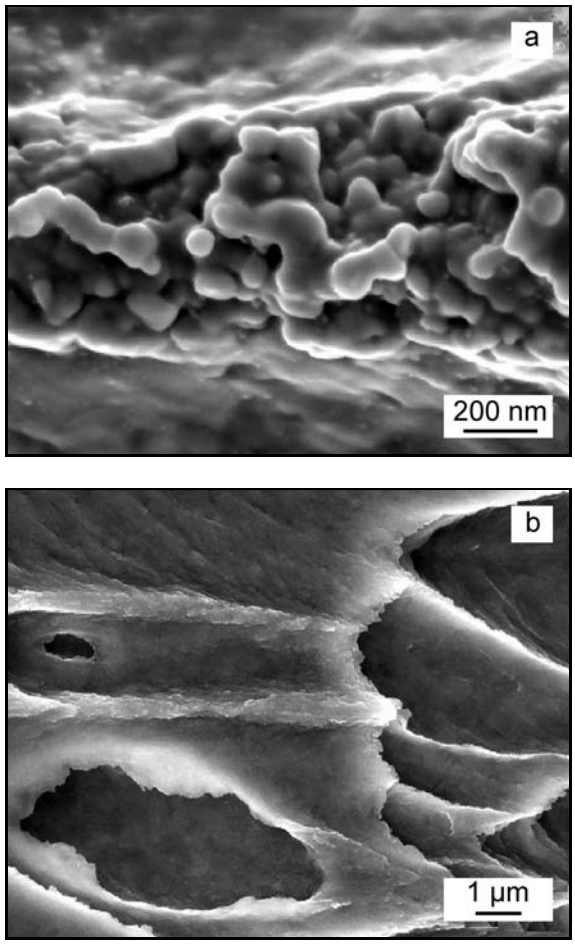

Fig. 8. High resolution SEM image of the rough wall between two dimples of NS Ti fracture surface consisting from individual grains or their clusters (a), the detail of ragged dimple walls perforation on sample fractured at 77 K (b).

is displayed in Figs. 6b, 7b and in a detail in Fig. 8b. This feature is not present on the smooth walls where the temperature increase was sufficient to change the original nanostructural character of material microstructure. A similar perforation of the nanostructured film formed inside dimple walls of nanocrystalline Ni-Fe alloys was observed by Li et al. [13]. Smooth oval shape of perforations may be an indication that they are formed due to the surface tension forces in sufficiently hot dimple wall during tensile elongation.

4. Conclusions

The Equal Channel Angular Pressing method makes it possible to obtain bulk nanostructural titanium, which can be regarded as a potential structural material for cryogenic applications. The yield stress of nanostructured titanium increases with decreasing temperature and with decreasing grain size. The analyses of failure and morphology of fracture surfaces of nanostructured titanium lead to the following conclusions:

– At low temperatures the failure of nanostructured titanium under uniaxial compression is due to the propagation of unstable plastic shear, which is accompanied by local adiabatic heating of the material. The shear band begins to propagate because of local inhomogeneities or deformation conditions. Inside the adiabatic shear band area, the shear deformation is very severe and identification of either microstructure and/or crack initiation becomes impossible.

– The fracture surface of NS titanium specimens is characterized by a modulation of the regions of elongated dimples without any manifestation of its nucleation on second phase particles and the regions with a relatively flat and smeared appearance.

– Two types of veins are usually observed on the one fracture surface – smooth veins and veins with rough ridges. The smooth veins are similar to these observed at fracture surface of bulk amorphous metallic alloys failed under similar conditions. On the rough veins the individual nanosized grains and their clusters could be observed. Specific vein pattern and its analysis help us to estimate that the local heating temperature did not overcome the recrystallization temperature (about 800 °C).

Unlike bulk metallic glasses, the fracture surface of NS titanium pints only occasionally at local melting (only few solidified melt drops were found). This is due to the high melting temperature of titanium (1668 °C), much higher than that of metallic glasses.

Acknowledgements

This work was partially supported by the Grant Agency for Science of Slovak Republic VEGA No. 2/0080/08.

References

[1] TIMOTHY, S. P.: Acta Metallurgica, *35*, 1987, p. 301.
[2] TABACHNIKOVA, E. D.—BENGUS, V. Z.—STOLYAROV, V. V.—RAAB, G. I.—VALIEV, R. Z.—CSACH, K.—MISKUF, J.: J. Mater. Sci. & Eng. A, *309–310*, 2001, p. 524.
[3] STAKER, M. R.: Acta Metallurgica, *29*, 1981, p. 683.
[4] MATTHEWS, D. T. A.—OCELÍK, V.—BRONSVELD, P.—DE HOSSON, J. TH. M.: Acta Materialia, *56*, 2008, p. 1762.
[5] BENGUS, V. Z.—TABACHNIKOVA, E. D.—SHUMILIN, S. E.—GOLOVIN, Y. I.—MAKAROV, M. V.—SHIBKOV, A. A: Int. J. Rapid Solidif., *8*, 1993, p. 21.

[6] BENGUS, V. Z.—TABACHNIKOVA, E. D.—NATSIK, V. D.—MIŠKUF, J.—CSACH, K.—STOLYAROV, V. V.—VALIEV, R. Z.: The Physics of Metals and Metallography, *94* (Suppl. 2), 2002, p. S11.
[7] KOVALEVA, V. N.—MOSKALENKO, V. A.—NATSIK, V. D.: Phil. Mag., *A70*, 1994, p. 423.
[8] LEVINE, E. D.: Transaction of the Metallurgical Society AIME, *234*, 1966, p. 1558.
[9] LEE, D. G.—KIM, Y. G.—NAM, D. H.—HUR, S. M.—LEE, S.: Mater. Sci. Eng. A, *391*, 2005, p. 221.
[10] XI, X. K.—ZHAO, D. Q.—PAN, M. X.—WANG, W. H.—WU, Y.—LEWANDOWSKI, J. J.: Phys. Rev. Lett., *94*, 2005, p. 125510.
[11] TABACHNIKOVA, E. D.—PODOLSKIY, A. V.—BENGUS, V. Z.—SMIRNOV, S. N.—CSACH, K.—MIŠKUF, J.—SAITOVA, L. R.—SEMENOVA, I. P.—VALIEV, R. Z.: Strength of Materials, *40*, 2008, p. 71.
[12] BENGUS, V. Z.—TABACHNIKOVA, E. D.—MIŠKUF, J.—CSACH, K.—OCELÍK, V.—JOHNSON, W. L.—MOLOKANOV, V. V.: J. Mater. Sci., *35*, 2000, p. 4449.
[13] LI, H.—EBRAHIMI, F.—CHOO, H.—LIAW, P. K.: J. Mater. Sci., *41,* 2006, p. 7636.